Mickelson, K. E., & Petra, P. H. (1978) *J. Biol. Chem. 253*, 5293-5298.
Moore, J. W., & Bulbrook, R. D. (1988) *Oxford Rev. Reprod. Biol. 10*, 181-236.
Örstan, A., Lulka, M. F., Eide, B., Petra, P. H., & Ross, J. B. A. (1986) *Biochemistry 25*, 2686-2692.
Paoletti, J., LePecq, J. B. (1969) *Anal. Biochem. 31*, 33-41.
Petra, P. H., & Lewis, J. (1980) *Anal. Biochem. 105*, 165-169.
Petra, P. H., Stanczyk, F. Z., Namkung, P. C., Fritz, M. A., & Novy, M. J. (1985) *J. Steroid Biochem. 22*, 739-746.
Petra, P. H., Kumar, S., Hayes, R., Ericsson, L. H., & Titani, K. (1986a) *J. Steroid Biochem. 24*, 45-49.
Petra, P. H., Namkung, P. C., Senear, D. F., McCrae, D. A., Rousslang, K. W., Teller, D. C., & Ross, J. B. A. (1986b) *J. Steroid Biochem. 25*, 191-200.
Plymate, S. R., Namkung, P. C., Matej, L. A., & Petra, P. H. (1990) *J. Steroid Biochem. 36*, 311-317.
Rosner, W., Toppel, S., & Smith, R. N. (1974) *Biochim. Biophys. Acta 351*, 92-98.
Ross, J. B. A., Rousslang, K. W., & Brand, L. (1981) *Biochemistry 20*, 4361-4369.
Ross, J. B. A., Torres, R., & Petra, P. H. (1982) *FEBS Lett. 149*, 240-244.
Ross, J. B. A., Contino, P. B., Lulka, M. F., & Petra, P. H. (1985) *J. Protein Chem. 4*, 299-304.
Sakiyama, R., Pardridge, V. M., & Musto, N. A. (1988) *J. Clin. Endocrinol. Metab. 67*, 98-103.
Stern, O., & Volmer, M. (1919) *Phys. Z. 20*, 183-188.
Vermeulen, A. L., Verdonck, L., Van der Straeten, M., & Orie, M. (1969) *J. Clin. Endocrinol. Metab. 29*, 1470-1480.
Weber, G. (1952) *Biochem. J. 51*, 155-167.
Weber, G. (1953) *Adv. Protein Chem. 8*, 514-549.
Westphal, U. (1986) *Steroid-Protein Interactions II, Monogr. Endocrinol. 27*.

Estimating the Contribution of Engineered Surface Electrostatic Interactions to Protein Stability by Using Double-Mutant Cycles†

Luis Serrano, Amnon Horovitz, Boaz Avron, Mark Bycroft, and Alan R. Fersht*
MRC Unit for Protein Function and Design, University Chemical Laboratory, Lensfield Road, Cambridge CB2 1EW, U.K.
Received February 14, 1990; Revised Manuscript Received May 8, 1990

ABSTRACT: Coulombic interactions between charges on the surface of proteins contribute to stability. It is difficult, however, to estimate their importance by protein engineering methods because mutation of one residue in an ion pair alters the energetics of many interactions in addition to the coulombic energy between the two components. We have estimated the interaction energy between two charged residues, Asp-12 and Arg-16, in an α-helix on the surface of a barnase mutant by invoking a double-mutant cycle involving wild-type enzyme (Asp-12,Thr-16), the single mutants Thr → Arg-16 and Asp → Ala-12, and the double mutant Asp → Ala-12,Thr → Arg-16. The changes in free energy of unfolding of the single mutants are not additive because of the coulombic interaction energy. Additivity is restored at high concentrations of salt that shield electrostatic interactions. The geometry of the ion pair in the mutant was assumed to be the same as that in the highly homologous ribonuclease from *Bacillus intermedius*, binase, which has Asp-12 and Arg-16 in the native enzyme. The ion pair does not form a hydrogen-bonded salt bridge, but the charges are separated by 5-6 Å. The mutant barnase containing the ion pair Asp-12/Arg-16 is more stable than wild type by 0.5 kcal/mol, but only a part of the increased stability is attributable to the electrostatic interaction. We present a formal analysis of how double-mutant cycles can be used to measure the energetics of pairwise interactions.

Electrostatic interactions are of fundamental and ubiquitous importance in binding, catalysis, protein folding, and the assembly of macromolecules (Perutz, 1978; Warshel & Russell, 1984). Special attention has been paid to the role of electrostatic interactions in stabilizing α-helices (Hol, 1985; Sali et al., 1988; Serrano & Fersht, 1989; Nicholson et al., 1988; Marqusee et al., 1987). Two types of electrostatic interactions in particular have been analyzed: charged residues with the helix dipole (Sali et al., 1988; Serrano & Fersht, 1989; Nicholson et al., 1988) and the interaction of charged residues within the helix (Nicholson et al., 1988; Marqusee et al., 1987). While several analyses indicate a value of 1.5-2.0 kcal/mol for the charge–helix dipole interaction, no quantitative values have been found for exposed charge–charge interactions on the surface of a helix, although qualitative evidence has been presented by Baldwin and co-workers (Nicholson et al., 1988; Marqusee et al., 1987). The small ribonuclease from *Bacillus amyloliquefaciens*, barnase (Hartley, 1989), has proved to be an excellent system for determining with high precision the energetics of interactions responsible for protein stability (Sali et al., 1988; Serrano & Fersht, 1989; Kellis et al., 1988, 1989). The enzyme of M_r 12 382 consists of a single polypeptide chain with no disulfide cross-links (Mauguen et al., 1982). It undergoes reversible unfolding induced either thermally or by solvents. Measurements of the energetics of unfolding of wild-type and mutant proteins may be used to quantify energies of interaction between side chains (Kellis et al., 1988, 1989) or long-range electrostatic interactions (Sali et al., 1988; Serrano & Fersht, 1989). Identical results are found from

† L.S. is an EMBO Fellow. A.H. and B.A. were funded by the Rothschild Foundation.

0006-2960/90/0429-9343$02.50/0

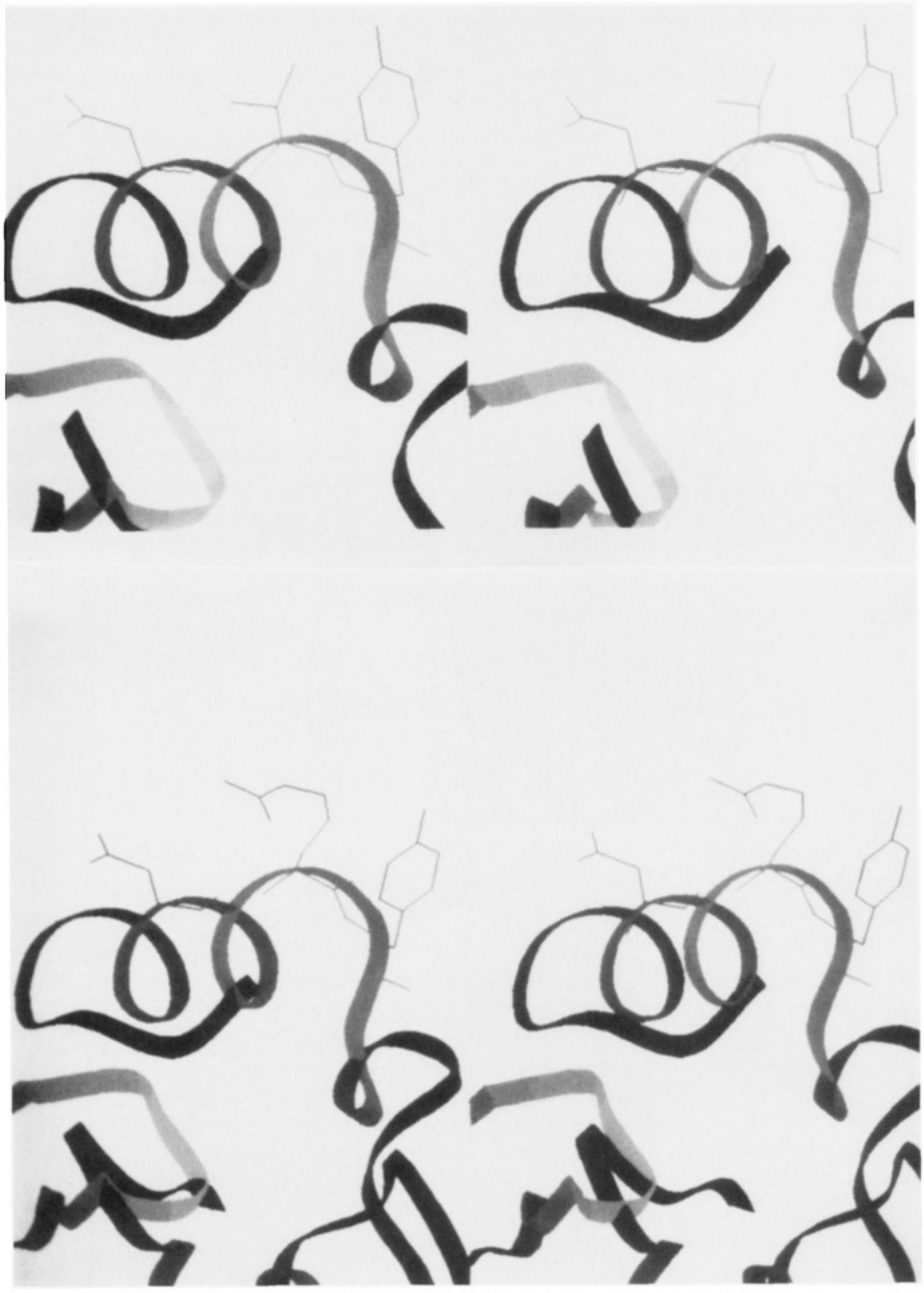

FIGURE 1: Top: Stereoview of barnase first α-helix with the residues of interest. (The coordinates for barnase were kindly provided by Professor G. Dodson and Dr. C. Hill). Bottom: Stereoview of binase first α-helix with the residues of interest.

unfolding induced by urea, guanidinium chloride, or heat (Kellis et al., 1989), showing that the results are not a function of the method of denaturation. Barnase has two helices (Mauguen et al., 1982; Hill et al., 1983); one consists of residues 6–18 and the other of residues 26–34. Asp-8 and Asp-12 in the first helix interact directly with Arg-110 (Figure 1). Barnase has an almost identical counterpart, binase from *Bacillus intermedius*, which is homologous for all but 12 residues (Hill et al., 1983; Pavlovsky et al., 1983; Sanishvili, 1989) and whose three-dimensional structure has been determined (Hill et al., 1983; Pavlovsky et al., 1989). In the first helix of binase, the charged residues Asp-8 and Asp-12 are present with the same geometry as in barnase (Figure 1) but there is an arginine at position 16, instead of the threonine. We have chosen to look at the interaction in barnase between Asp-12 and an arginine introduced at position 16 [the mutant barnase(Thr → Arg-16)] because we know by analogy with binase the structure of the enzyme at the relevant position. We report here NMR experiments that are consistent with the conformation of Arg-16 in barnase(Thr → Arg-16) being the same as that in binase.

Electrostatic interactions between charged groups and the active-site histidine of subtilisin were measured by mutating the charged groups and measuring the change in the pK_a of the histidine (Thomas et al., 1985, 1987; Russell & Fersht, 1987). These measurements were relatively straightforward because the only effects measured were those resulting from changes in long-range electrostatic interactions. The same is not true for measuring the coulombic interaction of, for example, a surface ion pair in a helix by simply mutating one of the pair of charges and measuring the change in stability of the protein. This is because on mutating a residue one changes a number of interactions within the protein, each of which contributes to stability. The following interactions are changed in addition to the coulombic interaction between the ion pair: (i) electrostatic interactions between the target charged residue and all other charges of the protein, including the helix dipoles; (ii) other noncovalent interaction energies

of the mutated residue with surrounding residues (hydrogen bonds, hydrophobic interactions, and (iii) interactions from any reorganization of the protein structure on mutation, including local conformational changes and repositioning of the unpaired partner of the electrostatic pair. We present here a method for estimating the coulombic interaction energy between two charged residues based on the double-mutant cycle of Carter et al. (1984) that was introduced to detect cooperative interactions between residues in the tyrosyl-tRNA synthetase and further analyzed by Horovitz (1986, 1987).

Experimental Procedures

Materials

The buffer used in the denaturation experiments was 2-[*N*-morpholino]ethanesulfonic acid (MES) from Sigma. The MES stock was a 1.00 M solution containing 387 mM acid form and 613 mM sodium salt, which gives a pH of 6.3 at 25 °C on dilution to 50 mM. Urea and guanidinium chloride were highly purified "Aristar" grade, from BDH Limited. Restriction enzymes and molecular biological reagents were obtained from New England Biolabs and Boehringer Mannheim, the radiochemicals were from Amersham International, and SP-Trisacryl was obtained from IBF. All other reagents were purchased from either Sigma or BDH Limited. *Escherichia coli* BL21DE3 pLysS was a generous gift from Dr. F. W. Studier. Plasmid pTZ18U and the helper phage M13KO7 were obtained from Pharmacia.

Wild-type barnase gene was cloned into the plasmid pUC19 by Paddon and Hartley (1987). This recombinant plasmid, pMT410, which confers resistance to ampicillin, was generously donated by Dr. Hartley. It contains the structural gene for barnase fused to the promoter and signal sequence of the *E. coli* alkaline phosphatase gene, as well as the gene for barstar (the intracellular inhibitor of barnase; Smeaton & Elliot, 1967) under the control of its own promoter. These genes are in a 1.4-kb *Eco*RI–*Hin*dIII restriction fragment. This restriction fragment was cloned on the pTZ18U plasmid (Pharmacia), previously digested with the same enzymes. This plasmid has an f1 origin of replication so it allows the production of ssDNA upon infection by a helper phage. It also has the T7 polymerase promoter before the *Eco*RI site.

Mutagenesis. Single-stranded DNA was obtained from the modified pTZ18U, harbored in *E. coli* TG2 after infection with the helper phage M13KO7 (Pharmacia), following the conditions described by Pharmacia. Site-directed mutagenesis was carried out by using the method of Eckstein (Sayers & Eckstein, 1988) and the kit supplied by Amersham (using $^1/_5$ of the recommended amounts of DNA and kit). The following oligonucleotides were used:

Asp → Ala-12:
5′-GTCTGAAGATAAG*CCGCAACCCC-3′

Thr → Arg-16: 5′-GCTTATGATATC*T*CTGAAG-3′

Asp → Ala-12 on Arg-16 template:
5′-CTCTGAAGATAAG*CCGCAACCCC-3′

(an asterisk follows the mismatched base).

Mutants were identified by direct sequencing of ssDNA. The mutant DNA was used to transfect the BL21DE3 (F^-, *ompT*, r_B^-, m_B^-) (Grodberg & Dunn, 1988; Studier & Moffatt, 1986) strain of *E. coli*. This strain harbors the pLysS plasmid that confers chloramphenicol resistance and constitutively expresses the T7 lysozyme (Chang & Cohen, 1978). The BL21DE3 strain contains the gene for the T7 polymerase under the control of the *lac*UV5 promoter (Studier & Moffatt, 1986).

Production of Barnase. A 30-mL starter culture of *E. coli* containing the wild-type or mutant plasmid was grown overnight in Luria broth (Lennox, 1955) containing 50 μg of ampicillin/mL and 25 μg of chloramphenicol/mL. This culture was used to inoculate 1 L of low-phosphate medium (Serpersu et al., 1986) containing ampicillin and chloramphenicol. Phosphate starvation leads to activation of the alkaline phosphatase promoter and, consequently, synthesis and secretion of barnase. Cells were grown for 18 h at 30 °C in Erlenmeyer flasks, with vigorous shaking, before being harvested. Barnase was purified by a method adapted from Paddon and Hartley (1987) (Mossakowska et al., 1989). The culture medium was chilled to 4 °C, and 55 mL of glacial acetic acid/L of culture was slowly added while stirring. The acidification releases additional barnase from the periplasm into the medium (R. W. Hartley, personal communication). Stirring was continued for 15 min. The culture was centrifuged for 15 min at 10000*g* to pellet the cells. The supernatant fluid was combined with 5 mL of SP-Trisacryl cation-exchange resin that had been previously washed with 50 mM sodium acetate, pH 5.0 ("equilibration buffer"). Barnase was allowed to adsorb to the resin for 1 h with gentle swirling. The resin was allowed to settle, and the supernatant fluid was decanted. The resin was washed several times with equilibration buffer and then poured into a chromatography column. The column was washed with equilibration buffer until A_{280} of the eluate was negligible. Barnase was eluted from the column with equilibration buffer containing 0.5 M NaCl. The eluted protein was dialyzed overnight in M_r = 3500 cutoff dialysis tubing (Spectrum Medical Industries, Inc.) against equilibration buffer. The final purification step was carried out at ambient temperature with a Pharmacia FPLC system using a Mono-S cation-exchange column. Barnase was bound to the column in equilibration buffer and was eluted approximately halfway through a linear gradient of 0–0.4 M NaCl. Purified barnase was dialyzed overnight against double-distilled water, flash frozen, and stored at −70 °C. The recovery of purified barnase varied from roughy 1 to 10 mg/L of culture, with less stable mutants giving lower yields. The purified proteins were homogeneous as judged by $NaDodSO_4$–polyacrylamide gel electrophoresis.

Methods

Unfolding was monitored by fluorescence spectroscopy (Hartley, 1975) with excitation at 290 nm and emission at 315 nm (Kellis et al., 1989). The intrinsic fluorescence of barnase decreases by 80% upon unfolding. The urea solutions were prepared as before (Kellis et al., 1989), frozen in dry ice, and stored at −20 °C to minimize the formation of ammonium cyanate on storage. For each point on the denaturation profile, 100 μL of 9 μM barnase in 450 mM MES was diluted into 800 μL of the appropriate denaturant solution and incubated at 25 °C for approximately 1–3 h. The extent of unfolding is constant from a few seconds to 8 h. Fluorometric measurements were made in thermostated cuvette holders at 25.0 °C. The temperature was carefully monitored by a thermocouple immersed in the cuvette above the light beam. Unfolding is completely reversible as shown by diluting samples of unfolded protein to low urea concentration and measuring the recovery of fluorescence (Kellis et al., 1989).

Analysis of Urea Denaturation. Denaturation of Wild-Type Enzyme. The equilibrium constant for unfolding, K_u, in the presence of a denaturant is calculated from eq 1 where F is

$$K_u = (F_F - F)/(F - F_U) \quad (1)$$

the observed fluorescence and F_F and F_U are the values of the

fluorescence of the folded and unfolded forms of the protein. The transition corresponds to a two-state process (Hartley, 1989). The values of F_F and F_U during urea-induced denaturation are independent of the concentration of urea up to 6.5 M, and so eq 1 is simply applied (Kellis et al., 1989). It has been found experimentally that the free energy of unfolded proteins in the presence of urea is linearly related to the concentration of the denaturant (Pace, 1986):

$$\Delta G_U = \Delta G_{H_2O} - m[\text{denaturant}] \quad (2)$$

The value of m and ΔG_{H_2O}, the apparent free energy of unfolding in the absence of denaturant, may be calculated from eq 1, because $\Delta G_{H_2O} = -RT \ln K_U$. We directly fit the entire data set from the fluorescence-monitored urea denaturation with the nonlinear regression analysis program Enzfitter (published by Elsevier-Biosoft, Cambridge, U.K.) by using eq 3 (which is derived from eqs 1 and 2). There is a long

$$F = F_F - (F_F - F_U) \exp\{(m[\text{urea}] - \Delta G_{H_2O})/RT\}/\{1 + \exp[(m[\text{urea}] - \Delta G_{H_2O})/RT]\} \quad (3)$$

extrapolation to 0 M urea from measurements made over the range 4.0–5.0 M urea. Consequently, small errors in m result in large errors in the estimation of ΔG_{H_2O}. On the other hand, it is found that the concentration of denaturant at 50% unfolding ($[\text{urea}]_{50\%}$) is very reproducible (Kellis et al., 1989). This quantity can be used for determining $\Delta\Delta G_{H_2O}$ between wild-type and mutant proteins by using eq 4, where $\Delta[\text{urea}]_{50\%}$

$$\Delta\Delta G_{H_2O} = \langle m \rangle \Delta[\text{urea}]_{50\%} \quad (4)$$

is the difference between the value of $[\text{urea}]_{50\%}$ for wild-type and mutant and $\langle m \rangle$ is the average value of m (Kellis et al., 1989; Serrano & Fersht, 1989). This is a precise way to compare stabilities of modified proteins provided m is constant within experimental error (Cupo & Pace, 1983; Kellis et al., 1989). If the value of m changes on mutation, then the observed value of $\Delta\Delta G$ calculated from eq 4 is the value that holds for the concentration of urea midway between the values of $[\text{urea}]_{50\%}$ for the two proteins—see Appendix.

NMR Methods. NMR spectra were acquired on a Bruker AM 500 spectrometer with an Aspect 3000 computer by using procedures detailed by Bycroft et al. (1990). Spectra were recorded at 37 °C and pH 4.5. COSY (Aue et al., 1976; Bax & Freeman, 1981) and NOESY (Jeener et al., 1979; Kumar et al., 1980) experiments were recorded with 2048 data points in t_2 and 512 t_1 increments with a spectral width of 8000 Hz in both dimensions. A relaxation delay of 1.5 s was used. Suppression of the solvent signal was achieved by presaturation of the water resonance during the relaxation delay.

Results

Values of ΔG_{H_2O}, m, and the urea concentration at which half of the protein is denatured, $[\text{urea}]_{50\%}$, for wild-type protein are given in Table I. The average value of m obtained from the data collected from different preparations of protein and analyzed with different batches of urea is 2.17, with a spread of ±8% (standard error of mean = ± 2.2%, n = 9). Although reasonably accurate values of ΔG_{H_2O} may be derived from eq 2, the differences between the values obtained from different analyses of the wild-type protein lie in a range of ±10% as there is a long extrapolation to 0 M urea from measurements made over the range 4.0–5.0 M urea. However, even though ΔG_{H_2O} is not known accurately, $\Delta\Delta G_{H_2O}$ can be calculated with precision. This is because the value of $[\text{urea}]_{50\%}$ is reproducible to within a spread of ±0.25% (Table I; Kellis et al., 1989) and the value of $\Delta\Delta G_{H_2O}$ can be calculated from $[\text{urea}]_{50\%}$ by using eq 4. The uncertainty of ±0.25% in $[\text{urea}]_{50\%}$ is equivalent to ±0.022 kcal/mol [i.e., ±(0.01 M × 2.2 kcal M^{-1} mol^{-1})]. In the following discussion, values of ΔG_{H_2O} have a reliability of about ±1 kcal/mol, $\Delta[\text{urea}]_{50\%}$ ±0.01 M, $\Delta\Delta G_{H_2O}$ ±0.03 kcal/mol, and $\Delta\Delta G_{int}$ ±0.04 kcal/mol. Measurements of the denaturation of wild-type protein and each of the three mutant proteins at any one concentration of salt were performed on the same day with the same buffer solutions to minimize systematic errors in the measurement of $[\text{urea}]_{50\%}$. The variation of m over the range of salt concentrations appears to be random for each mutant protein, and the spread is similar to that found for experiments repeated on wild-type protein at constant reaction conditions (Tables I and II). The average value of m is in all cases within experimental error the same as that for wild-type protein [$m_{wildtype}$ = 2.18 ± 4% (this study); $m_{Ala\text{-}12}$ = 2.15 ± 8%; $m_{Arg\text{-}16}$ = 2.11 ± 7.5%; $m_{Ala\text{-}12,Arg\text{-}16}$ = 2.10 ± 9.5% (±standard error)].

Table I: Free Energy of Unfolding of Wild-Type Barnase Determined by Reversible Urea Denaturation[a]

ΔG_{H_2O}[b] (kcal/mol)	m[c] (kcal mol^{-1} M^{-1})	$[\text{urea}]_{50\%}$[d] (M)
10.93	2.39	4.58
10.16	2.22	4.58
10.15	2.22	4.57
10.66	2.33	4.56
10.15	2.22	4.57
9.55	2.09	4.57
9.42[e]	2.06	4.57
9.06[e]	1.98	4.57
9.45[f]	2.06	4.58

[a] The data are based on repeated measurements by different experimenters over a period of two years using different preparations of enzyme, buffers and urea. Denaturation was done at pH 6.3, 50 mM Na-Mes, and 25.0 °C with 1 μM protein as described under Experimental Procedures. [b] ΔG_{H_2O} was determined by extrapolation of the urea denaturation curve to 0 M urea. [c] m is the slope of the linear denaturation plot, $-d\Delta G_u/d[\text{urea}]$. [d] $[\text{urea}]_{50\%}$ is the concentration of urea at which 50% of the protein is unfolded. [e] Data supplied by J. T. Kellis, Jr. [f] Data supplied by D. Sali.

Increasing the concentration of salt increases the stability of the proteins; for example, the addition of 900 mM NaCl raises the value of $[\text{urea}]_{50\%}$ by over 1 M (Table II). At 10 mM buffer, the mutant Thr → Arg-16 has a value of $[\text{urea}]_{50\%}$ that is 0.22 M higher than wild type, which is equivalent to an increase in stability of 0.48 kcal/mol. The value of ΔG_{H_2O} for the mutant is lower than that for wild type, but this is because of experimental error in the long extrapolation and the uncertainty in m. At 50 mM buffer, which is the standard buffer for our studies and where the most accurate measurements of ΔG_{H_2O} and m were made, that mutant has a raised value of $[\text{urea}]_{50\%}$ of 0.24 M (equivalent to 0.52 kcal/mol), and ΔG_{H_2O} found from extrapolation to 0 M urea is higher than for wild type by 0.48 kcal/mol.

The changes in free energy of unfolding are understood most simply from a series of double-mutant cycles (Figure 2). At ionic strength 0.01 M, the Thr → Arg-16 mutant, which contains the ion pair, is more stable than wild type by 0.48 kcal/mol. Changing Thr → Arg-16 in the Asp → Ala-12 mutant to generate the double mutant Asp → Ala-12,Thr → Arg-16 increases the stability by only 0.15 kcal/mol (relative to Asp → Ala-12). There is a discrepancy of 0.33 kcal/mol in the two vertical mutations in the cycle, i.e., there is a coupling energy, $\Delta\Delta G_{int}$, of 0.33 kcal/mol. Mutating Asp → Ala-12 in wild type lowers the stability by 0.43 kcal/mol. Making the analogous mutation in the mutant Arg-16 lowers the stability by 0.76 kcal/mol. $\Delta\Delta G_{int}$ is, of course, also 0.33 kcal/mol for the horizontal arrows of the cycle. The value of $\Delta\Delta G_{int}$ decreases with increasing ionic strength until it is within experimental error of zero at ionic strength 0.9 M,

Table II: Changes in the Free Energies of Unfolding of Wild-Type Barnase, the Single Mutants Asp → Ala-12 and Thr → Arg-16, and the Double Mutant Asp → Ala-12, Thr → Arg-16 at Different Salt Concentrations Determined by Reversible Urea Denaturation[a]

salt concn	mutant	ΔG_{H_2O}[b] (kcal/mol)	m[c] (kcal mol^{-1} M^{-1})	[urea]$_{50\%}$[d] (M)	$\Delta\Delta G_u$[e] (kcal/mol)
10 mM Na-Mes	wild type	10.01	2.21	4.53	0.00
	Asp → Ala-12	10.12	2.33	4.33	0.43
	Thr → Arg-16	9.23	1.94	4.75	−0.48
	Asp → Ala-12,Thr → Arg-16	9.88	2.24	4.40	0.28
50 mM Na-Mes	wild type	10.15	2.22	4.57	0.00
	Asp → Ala-12	9.36	2.12	4.41	0.35
	Thr → Arg-16	10.63	2.21	4.81	−0.52
	Asp → Ala-12,Thr → Arg-16	10.00	2.20	4.55	0.04
50 mM Na-Mes	wild-type	10.37	2.20	4.71	0.00
50 mM NaCl	Asp → Ala-12	10.64	2.33	4.56	0.33
	Thr → Arg-16	10.21	2.06	4.94	−0.50
	Asp → Ala-12,Thr → Arg-16	10.40	2.19	4.75	−0.09
50 mM Na-Mes	wild type	10.88	2.10	5.20	0.00
500 mM NaCl	Asp → Ala-12	10.76	2.12	5.07	0.28
	Thr → Arg-16	10.55	1.95	5.40	−0.43
	Asp → Ala-12,Thr → Arg-16	11.14	2.11	5.29	−0.20
50 mM Na-Mes	wild type	12.90	2.15	5.64	0.00
900 mM NaCl	Asp → Ala-12	10.65	1.93	5.53	0.24
	Thr → Arg-16	12.90	2.21	5.84	−0.43
	Asp → Ala-12,Thr → Arg-16	10.89	1.90	5.74	−0.22

[a] Denaturation was performed as described under Experimental Procedures. [b] ΔG_{H_2O} was determined by urea denaturation of the proteins and extrapolation of the data to zero denaturation. [c] m is the slope of the linear denaturation plot, $-d\Delta G_u/d[urea]$. [d] [urea]$_{50\%}$ is the concentration of urea at which 50% of the protein is unfolded. [e] $\Delta\Delta G_u$ was determined by multiplying the Δ[urea]$_{50\%}$ value by the average slope $\langle m \rangle$ (=2.17)—see Appendix.

Table III: Interatomic Distances between Tyr-17 and Thr-16 in Barnase and Arg-16 in Binase

	Tyr-17					
	C_β	$C_{\delta 1}$	$C_{\delta 2}$	$C_{\epsilon 1}$	$C_{\epsilon 2}$	C_ζ
Thr-16 C_β	4.3	4.5	4.0	4.5	4.0	4.3
Arg 16 C_β	4.2	4.7	3.8	4.9	4.0	4.6
Thr-16 C_γ	4.7	4.4	4.5	4.1	4.1	3.9
Arg-16 C_γ	4.2	4.3	3.9	4.1	3.7	3.8
Arg-16 C_δ	4.9	5.0	4.2	4.4	3.5	3.7

Table IV: Interatomic Distances between Thr-16 in Barnase and Arg-16 in Binase and Asp-12 and Arg-110

		Asp-12			Arg-110	
		$O_{\delta 1}$	$O_{\delta 2}$	CO	N_{H1}	N_{H2}
Arg-16	N_{H1}	6.8	6.1	4.1	8.9	11.1
	N_{H2}	5.6	5.0	4.3	7.9	10.1
	N_ϵ	7.4	7.1	4.6	9.8	11.8
Thr-16	$O_{\gamma 1}$	5.9	6.9	2.7	9.0	10.5
	$C_{\gamma 2}$	8.2	9.0	4.8	11.4	13.0

where $\Delta\Delta G_{int} = -0.03 \pm 0.04$ kcal/mol.

Comparison of Structural Interactions in the First Helix of Barnase and Binase. Interpretation of the above data requires structural information on the effects of mutation. This was done initially for the mutant with the Asp-12/Arg-16 ion pair by using the known structure of binase, which contains that ion pair. The C_β methylene and $C\gamma$ methyl group of Thr-16 of barnase make hydrophobic interactions with Tyr-17 (Table III), while the γ OH makes a hydrogen bond with the main-chain CO of Asp-12 (Figure 1). The C_β and C_γ methylene groups of Arg-16 in binase have similar conformations to those of Thr-16 in barnase and so make the same contacts with Tyr-17 (Table III). There are, however, extra contacts made by the C_δ of Arg-16 with Tyr-17 (Table III). One of the two $-NH_2$ groups of the side-chain of Arg-16 points toward the main-chain CO group of Asp-12 while the other one points toward the side chain of Asp-12 (Figure 1). The $-NH_2$ group of Arg-16 and the main-chain CO group of Asp-12 have the correct geometry for hydrogen-bond formation, but the N–O distance is rather long at 4 Å (Table IV). However, the map of binase is not highly refined and so a hydrogen bond cannot be ruled out. The side chain of Arg-16 is too far from the carboxylate of Asp-12 to make what is generally considered to be a salt bridge (i.e., positively and negatively charged hydrogen-bond donor and acceptor within hydrogen-bonding distance) (Table IV). The separation of some 6 Å is, however, sufficiently close that there could be a significant electrostatic interaction.

Structure of Barnase(Thr → Arg-16). As binase and barnase have almost identical three-dimensional structures (rms deviation of the main-chain α-carbons = 0.513 Å; Hill et al., 1983), it is reasonable to assume that Arg-16 in barnase(Thr → Arg-16) has the same conformation as Arg-16 in binase. However, barnase and binase differ in two other neighboring residues: Gln-15 and His-18 in barnase are Ile-15 and Lys-18 in binase. To check the local conformation in the helix, we analyzed barnase(Thr → Arg-16) by ^{1}H NMR, greater than 99% of the protons of barnase having been previously assigned (Bycroft et al., 1990). Comparison of 500-MHz 2D NMR COSY and NOESY spectra of the mutant with those of wild-type (M. Bycroft, unpublished data) reveals that changes in chemical shift of greater than 0.1 ppm occur only within a few angstroms of the site of mutation, indicating that no large structural change occurs on mutation of Thr → Arg-16. There are no changes in chemical shift of residues in the first helix before residue 11. Residues 12, 13, and 15–18 all have changes in backbone resonances greater than 0.1 ppm. These changes, 0.1–0.5 ppm, are significantly above noise and are consistent with the side chain of Arg-16 interacting with the residues in the adjacent turns of the helix. Chemical shifts are sensitive to electrostatic effects and so the changes are consistent with the presence of the positively charged arginine side chain. For Asp-12, the changes in chemical shift are larger for the backbone than for the C_β protons. This suggests that the positive charge on the arginine is not close to the carboxylate of Asp-12 and is consistent with the absence of an intimate salt bridge between Asp-12 and Arg-16. In the crystal structure of native barnase, the γ methyl of Thr-16 interacts with the ring of Tyr-17 and a NOE interaction is observed between the associated protons. In the Thr → Arg-16 mutant, the chemical shifts of the ring protons of Tyr-17 are essentially unchanged and a NOE is observed between the C_β

protons of Arg-16 and the C_δ protons of Tyr-17. This indicates that there is an interaction between the side chains of Arg-16 and Tyr-17 in the mutant that is similar to that between Thr-16 and Tyr-17 in wild type. All these data are consistent with the conformation of Arg-16 in barnase(Thr → Arg-16) being identical with that of binase.

Discussion

The electrostatic interaction between two residues in a protein, such as Asp-12 and Arg-16 in the barnase mutant, cannot be measured by simply mutating one of them, e.g., Arg → Thr-16, and measuring the difference in free energy of unfolding because too many interactions are simultaneously changed. These include the electrostatic interactions of Arg-16 with all other charges of the protein, including the macroscopic dipole of the α-helix, the probable hydrogen bond between an NH^+ of the side chain and the backbone CO of Asp-12; changes in other noncovalent interaction energies of the side chain with surrounding residues (the C_γ carbon of Thr-16, for example, has a hydrophobic interaction with the ring of Tyr-17 that is worth 1.9 kcal/mol; Matouschek et al., 1989), and any energetics of reorganization of the protein structure on mutation. We have been able to isolate the energy of the electrostatic interaction between Arg-16 and Asp-12 by using a double-mutant cycle in which Asp-12 and Arg-16 are mutated separately and together (see Figure 2). A formal analysis of the double-mutant cycle is given in the Appendix but the principles are straightforward. The change in free energy of unfolding is measured on mutation of, say, Arg → Thr-16 in the enzyme containing both Arg-16 and Asp-12. The measurement is repeated on the enzyme in which Asp-12 has been mutated already to an alanine. Intuitively, the difference in unfolding energy on changing Arg → Thr-16 in the Asp-12/Arg-16 enzyme and Arg → Thr-16 in the Ala-12/Arg-16 enzyme is the electrostatic interaction energy between the charges on Arg-16 and Asp-12 (G_{X^+/Y^-es}). The difference in energies is $\Delta\Delta G_{int}$, the coupling energy between the two residues. This coupling energy is not, however, necessarily equal to the coulombic energy of the ion pair. In order for G_{X^+/Y^-es} to equal $\Delta\Delta G_{int}$, it must be shown that (i) the nonelectrostatic components of this interaction are additive and (ii) that the local charged residues do not move on mutation and so change their coulombic interaction energies. There is a good control for the nonelectrostatic component since, at high salt concentrations, electrostatic interactions are masked and so only the nonelectrostatic components are measured. It is, indeed, found that the coupling energy at the high salt concentration is indistinguishable from zero at -0.03 ± 0.04 kcal/mol compared with 0.33 kcal/mol at the low salt concentration (Figure 2), and so the nonelectrostatic components of the cycle are additive (see also Table II). The most likely charged residue to move on mutation is the partner in the ion pair. The experiment was designed to minimize this likelihood since both components of the ion pair have multiple interactions elsewhere in the protein: e.g., Arg-16 interacts with the protein backbone and Asp-12 forms a tight salt bridge with Arg-110. We knew from the structure of binase that the position of Asp-12 does not change upon mutation of the partner in the ion pair. This was confirmed by NMR. Further, the position of Arg-110 is also anchored; its guanidinium moiety makes a good salt bridge with Asp-8 in the helix so that Arg-110 is constrained on mutation of Asp-12.

As discussed in the Appendix, the measurements give the difference in energy between the folded and unfolded states of the protein. There is direct experimental evidence that the C-terminus of the helix spanning residues 12–16 is unfolded in urea. First, NMR experiments on the unfolded state in urea fail to detect residual structure. Second, other mutational experiments on the helix show that the C-terminus is disrupted: mutation of residues Thr → Ser-16 loses all of the energy of interaction between the γ methyl of Thr-16 and the aromatic ring of Tyr-17 in the helix, and mutation of His → Gln-18 removes the electrostatic interaction between it and the C-terminus of the helix spanning residues 8–18 (Matouschek et al., 1989; Sali et al., 1988).

The apparent dielectric constant of the protein between Arg-16 and Asp-12 can be calculated from Coulomb's law and the measured interaction energy. Assuming that each of the two oxygen atoms of the Asp-12 side-chain has half a negative charge, and that each of the three NH groups of Arg-16 has one-third of a positive charge, we calculate a value of approximately 150 for the dielectric constant in 4 M urea at ionic strength 0.01 M, about double that for water. Urea (4 M) has a small effect on the macroscopic dielectric constant of water, raising it from 78.5 to 88 (Hartmann et al., 1967). Previous measurements of effective dielectric constants in different regions of subtilisin have given values ranging between 50 and 120 for exposed charges located between 10 and 25 Å from each other (Russell et al., 1987). Theoretical calculations based on subtilisin indicate that the effective dielectric constant between a charge and a point of interest depends on their relative positions in the protein (Fersht & Sternberg, 1989). Arg-16 and Asp-12 are located in a highly charged environment, with three charged residues in close proximity (Asp-8, His-18, and Arg-110). This could result in oriented water dipoles that could effectively raise the value of the dielectric constant in that area. The effect of ionic strength is also dramatic: the electrostatic interactions are masked at far lower concentrations of salt than found previously from the experiments on subtilisin.

The high effective local dielectric constant and the sensitivity to ionic strength render the interaction energy between Asp-12 and Arg-16 very small. The charges on these residues are separated by about 6 Å. These residues are in positions in a helix ($i,i+4$) that are optimal for making a true surface salt bridge, and a salt bridge can be readily modeled by computer graphics by moving Arg-16 while leaving Asp-12 bridged with Arg-110. Nevertheless, Arg-16 takes up an orientation where it makes other interactions. Surface salt bridges need not contribute greatly to stability, as their importance is context dependent.

Appendix: Measurement of Direct Electrostatic Effects and Other Pairwise Interactions from Changes in Unfolding Energies

It is of interest to know the interaction energy between two groups in a protein, or two groups in an enzyme–ligand complex, relative either to the absence of that interaction or to the interaction of each with water. Experiments on mutant enzymes, however, give, in general, measurements of interaction energies that correspond to the relative energetics of having one residue vis-a-vis another at a specific position. Such experiments always give a direct measurement of the specificity of an interaction or the relative stability of two enzymes but not the interaction energies (Fersht, 1987, 1988). We show that these energies may, in principle, be measured by double-mutant cycles. A general scheme for a double-mutant cycle is given in Figure 3 where E stands for enzyme, X and Y for the two target residues in the enzyme and $\Delta G_{E\text{-}XY\rightarrow E\text{-}X}$, $\Delta G_{E\text{-}Y\rightarrow E}$, $\Delta G_{E\text{-}XY\rightarrow E\text{-}Y}$, and $\Delta G_{E\text{-}X\rightarrow E}$ for the free energy changes of the appropriate transitions in the cycle. If the effects of the two mutations are independent, then identical

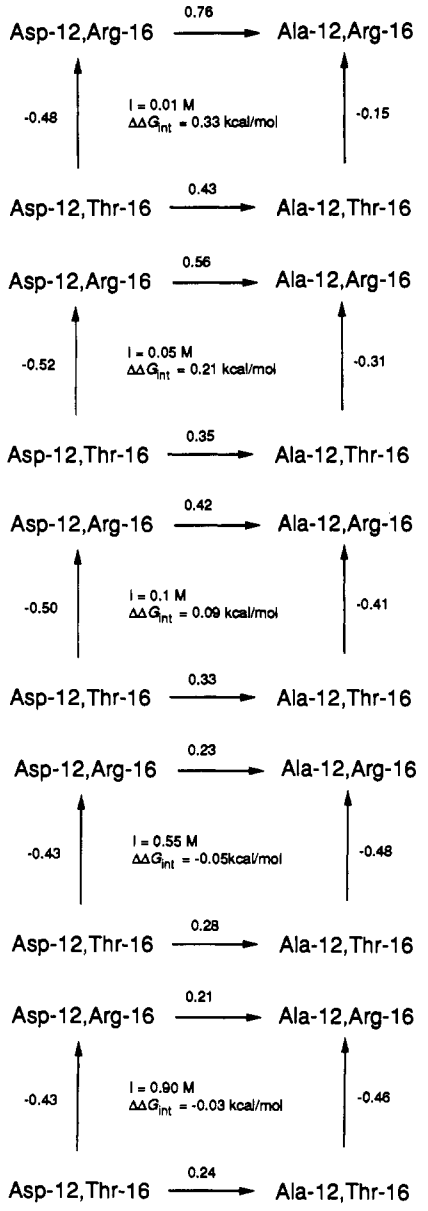

FIGURE 2: Double-mutant cycles for unfolding at various values of ionic strength. Wild-type barnase is at the bottom left of each cycle. Values of $\Delta\Delta G_{H_2O}$ are given by each arrow in units of kcal/mol. A negative sign means an increase in stability in direction of arrow. These values are for urea solutions of ~4.5–5 M. Many of the differences in energetics between water and urea solutions cancel out in the calculation of $\Delta\Delta G_{int}$—see Appendix—except that the value of $\Delta\Delta G_{int}$ is measured for the presence of urea. At the concentrations of urea in these experiments, the dielectric constant of the medium is raised by about 12% (Hartmann et al., 1967) so that values of $\Delta\Delta G_{int}$ are underestimated by 12% as these result from long-range electrostatic effects.

changes in energy are found upon making the same mutation in wild-type and mutant enzymes. If the mutations are not independent, then $\Delta G_{E\text{-}XY\rightarrow E\text{-}X} \neq \Delta G_{E\text{-}Y\rightarrow E}$ and $\Delta G_{E\text{-}XY\rightarrow E\text{-}Y} \neq \Delta G_{E\text{-}X\rightarrow E}$. The discrepancy is termed $\Delta\Delta G_{int}$, defined by

$$\Delta\Delta G_{int} = \Delta G_{E\text{-}XY\rightarrow E\text{-}X} - \Delta G_{E\text{-}Y\rightarrow E} = \Delta G_{E\text{-}XY\rightarrow E\text{-}Y} - \Delta G_{E\text{-}X\rightarrow E} \quad (A1)$$

$\Delta\Delta G_{int}$ is the coupling energy between the two residues. It may arise from direct interactions or be mediated by indirect effects propagated by changes in neighboring residues. We now analyze how direct electrostatic interactions may be separated from other energy changes.

The free energies in the above scheme are partitioned into individual components. The symbols are defined in Figure 3. The components interacting are indicated in the subscripts (e.g., $G_{X^+/solv}$ is the solvation energy of X^+; G_{E/X^+es} is the electrostatic energy between X^+ and E (apart from that with Y^-); G_E is the sum of the noncovalent energies within the protein and its solvent shell other than those directly involving X^+ and Y^-). A similar notation is used for the other changes. The differences in energy terms from one state to the next are defined by $\Delta G_{X^+/solv} = [G_{X^+/solv}]_2 - [G_{X^+/solv}]_1$, i.e., the change in solvation energy of X^+ on mutation of Y^- in E-X^+Y^-; $\Delta G_{E/X^+es} = [G_{E/X^+es}]_2 - [G_{E/X^+es}]_1$, i.e., the change in the electrostatic energy on mutation of Y^- in E-X^+Y^-; $\Delta G_{E/X^+nones} = [G_{E/X^+nones}]_2 - [G_{E/X^+nones}]_1$, i.e., the change in the non-electrostatic energy on mutation of Y^- in E-X^+Y^-; $\Delta G_{reorg(Y)} = [G_E]_2 - [G_E]_1$, i.e., the reorganization energy of E caused by any conformational changes on mutation of Y^- in E-X^+Y^-; $\Delta G'_{reorg(Y)} = [G_E]_4 - [G_E]_3$; $\Delta G_{reorg(X)} = [G_e]_3 - [G_E]_1$; $\Delta G'_{reorg(X)} = [G_E]_4 - [G_e]_2$. In the following analysis, we substitute the energies in states 2–4 by using the latter equations, and, for simplicity, the numerical subscript is dropped for the interactions in state 1.

The changes in free energy on mutating X and Y are given by

$$\Delta G_{E\text{-}XY\rightarrow E\text{-}X} = \Delta G_{X^+/solv} + \Delta G_{E/X^+es} + \Delta G_{E/X^+nones} - G_{X^+/Y^-es} - G_{E/Y^-es} - G_{E/Y^-nones} - G_{Y^-/solv} + \Delta G_{reorg(Y)} \quad (A2)$$

$$\Delta G_{E\text{-}Y\rightarrow E} = -G_{E/Y^-es} - \Delta G_{E/Y^-es} - G_{E/Y^-nones} - \Delta G_{E/Y^-nones} - G_{Y^-/solv} - \Delta G_{Y^-/solv} + \Delta G'_{reorg(Y)} \quad (A3)$$

$$\Delta G_{E\text{-}XY\rightarrow E\text{-}Y} = \Delta G_{Y^+/solv} + \Delta G_{E/Y^-es} + \Delta G_{E/Y^-nones} - G_{X^+/Y^-es} - G_{E/X^+es} - G_{E/X^+nones} - G_{X^+/solv} + \Delta G_{reorg(X)} \quad (A4)$$

$$\Delta G_{E\text{-}X\rightarrow E} = -G_{E/X^+es} - \Delta G_{E/X^+es} - G_{E/X^+nones} - \Delta G_{E/X^+nones} - G_{X^+/solv} - \Delta G_{X^+/solv} + \Delta G'_{reorg(X)} \quad (A5)$$

Subtracting eq A3 from A2 yields

$$\Delta\Delta G_{int} = \Delta G_{X^+/solv} + \Delta G_{E/X^+es} + \Delta G_{E/X^+nones} - G_{X^+/Y^-es} + \Delta G_{E/Y^-es} + \Delta G_{E/Y^-nones} + \Delta G_{Y^-/solv} + \Delta G_{reorg(Y)} - \Delta G'_{reorg(Y)} \quad (A6)$$

The identical equation is derived from eq A4 and A5 given that $\Delta G_{reorg(Y)} - \Delta G'_{reorg(Y)} = \Delta G_{reorg(X)} - \Delta G'_{reorg(X)} = [G_E]_3 + [G_E]_2 - [G_E]_4 - [G_E]_1$.

Case 1: Nondisruptive Mutations. Equation A6 (as well as eqs A2–A5) simplify greatly when the mutations are perfectly nondisruptive, i.e., neither X nor any other residue on the protein moves on the mutation of Y and conversely so. All the Δ terms in eq A6 are zero apart from $\Delta G_{Y^-/solv}$ and $\Delta G_{X^+/solv}$. The importance of the latter terms falls into two classes.

(*a*) *X and Y Are Separated by Solvent.* If X and Y are not in contact and are separately and independently solvated, then both $\Delta G_{Y^-/solv}$ and $\Delta G_{X^+/solv} = 0$. Equation A6 reduces to

$$\Delta\Delta G_{int} = -G_{X^+/Y^-es} \quad (A7)$$

That is, the interaction energy is the true coulombic energy between the ion pair.

(*b*) *X and Y Are in Contact.* If X and Y are in contact, their solvation must change on mutation as solvent takes the place of the missing contact on mutation. Then $\Delta G_{X^+/solv} \neq 0$ and $\Delta G_{Y^-/solv} \neq 0$. Then A6 gives

$$\Delta\Delta G_{int} = \Delta G_{X^+/solv} + \Delta G_{Y^-/solv} - G_{X^+/Y^-es} \quad (A8)$$

That is, the observed interaction energy is the difference in energy between the coulombic interaction energy between the charges on X and Y and the changes in their solvation energies

in the absence of each other. If solvent does not take the place of the missing contacts between X and Y, then $\Delta\Delta G_{int} = -G_{X^+/Y^-es}$. This is extremely unlikely, however, as partly desolvated charged residues are very unstable [see Fersht (1988)].

Case 2: Independent Mutations. If the mutations are predominantly nondisruptive but involve local minor reorganization of the enzyme, then there will be nonzero values of $\Delta G_{reorg(Y)}$ and $\Delta G_{reorg(X)}$. But if the local reorganizations are independent of each other (i.e., are entirely localized), then $\Delta G_{reorg(Y)} = \Delta G'_{reorg(Y)}$ and $\Delta G_{reorg(X)} = \Delta G'_{reorg(X)}$. These terms will cancel out in A6 and the final equation reduces to that for the purely nondisruptive examples.

Case 3: Dependent Mutations. If the mutation of Y causes X to move or vice versa, then X and Y occupy different positions in E-X and E-Y from E-XY. Mutations made from the single mutants to the double mutant means that terms in G and G' will not cancel and so values of the interaction energies will be complex.

Controls for Electrostatic Interactions. The terms involving electrostatic interactions can be eliminated by making measurements at high salt concentrations where charge–charge interactions become negligible, as found for subtilisin (Russell et al., 1987; Russell & Fersht, 1987). This affords a simple control because it can be readily seen if the nonelectrostatic energies are additive, that is, if $\Delta\Delta G_{int}$ is equal to zero at high concentrations of salt. Even if $(\Delta\Delta G_{int})_{highsalt}$ is not negligible, it can be used to interpret the changes at low ionic strengths. The coupling energy for the nonelectrostatic interactions at high salt is given by

$$(\Delta\Delta G_{int})_{highsalt} = \Delta G_{X^+/solv} + \Delta G_{E/X^+nones} + \Delta G_{E/Y^-nones} + \Delta G_{Y^-/solv} + \Delta G_{reorg(Y)} - \Delta G'_{reorg(Y)} \quad (A9)$$

If these non-electrostatic terms are the same at high salt as low salt, eq A9 may be subtracted from A6 to give

$$\Delta\Delta G_{int} - (\Delta\Delta G_{int})_{highsalt} = \Delta G_{E/X^+es} + \Delta G_{E/Y^-es} - G_{X^+/Y^-es} \quad (A10)$$

Crucial to the interpretation of eq A10 is the magnitude of the terms $\Delta G_{E/X^+es}$ and $\Delta G_{E/Y^-es}$, the changes in the coulombic energies of X and Y with the remainder of the enzyme on mutation of Y and X. These will be significant if there are major movements of charged residues on mutation. The residues most likely to move on mutation will be the remaining partners of the ion pair. Structural information is required on mutants to show that there not been significant movements of the charged residues on mutation. The mutations in this study were designed such that the partners in the ion pair do not move on mutation: the position of Asp-12 is constrained because it makes a closely constrained interaction with Arg-110, and the position of Arg-16 is constrained by interactions with Tyr-17 and a possible hydrogen bond with the backbone CO of Asp-12. Interestingly, when $\Delta G_{E/X^+es}$ and $\Delta G_{E/Y^-es}$ can be ignored

$$\Delta\Delta G_{int} - (\Delta\Delta G_{int})_{highsalt} = -G_{X^+/Y^-es} \quad (A11)$$

$\Delta\Delta G_{int} - (\Delta\Delta G_{int})_{highsalt}$ thus measures the coulombic interaction energy as in eq A8 even if the residues are in direct contact as in case 1b.

Extension of Analysis to Other Types of Interactions. It is a general phenomenon in measuring energetics from experiments on engineered mutants that measurements give interaction energies that are *apparent* values which are related to the true interaction energies (Fersht, 1987, 1988). The theory outlined above can give true interaction energies in other cases of pairwise interactions. For example, suppose X and Y are two residues that form a hydrogen bond with each other. Then we can set up a cycle as in Figure 3 with the following energy terms: $G_{X/solv}$ is the solvation energy of X, and $\Delta G_{X/solv}$ is the change in that energy on mutation of Y; $G_{E/X}$ is the interaction energy of X with E, and $\Delta G_{E/X}$ is the change in that energy on mutation of Y; $G_{X/Y}$ is the hydrogen-bond energy between X and Y; $\Delta G_{reorg(Y)}$ is the reorganization energy of E caused by any conformational changes on mutation of Y. A similar notation is used for the other changes as above.

$$\Delta G_{E\text{-}XY\rightarrow E\text{-}X} = \Delta G_{X/solv} + \Delta G_{E/X} - G_{X/Y} - G_{E/Y} - G_{Y/solv} + \Delta G_{reorg(Y)} \quad (A12)$$

$$\Delta G_{E\text{-}Y\rightarrow E} = -G_{E/Y} - \Delta G_{E/Y} - G_{Y/solv} - \Delta G_{Y/solv} + \Delta G'_{reorg(Y)} \quad (A13)$$

$$\Delta G_{E\text{-}XY\rightarrow E\text{-}Y} = \Delta G_{Y/solv} + \Delta G_{E/Y} - G_{X/Y} - G_{E/X} - G_{X/solv} + \Delta G_{reorg(X)} \quad (A14)$$

$$\Delta G_{E\text{-}X\rightarrow E} = -G_{E/X} - \Delta G_{E/X} - G_{X/solv} - \Delta G_{X/solv} + \Delta G'_{reorg(X)} \quad (A15)$$

Subtracting eq A13 from eq A12 gives

$$\Delta\Delta G_{int} = \Delta G_{X/solv} + \Delta G_{E/X} - G_{X/Y} + \Delta G_{E/Y} + \Delta G_{Y/solv} + \Delta G_{reorg(Y)} - \Delta G'_{reorg(Y)} \quad (A16)$$

For nondisruptive mutations, terms may be canceled as described in case 1b above to give

$$\Delta\Delta G_{int} = \Delta G_{X/solv} + \Delta G_{Y/solv} - G_{X/Y} \quad (A17)$$

The physical interpretation of A17 depends on the value of $\Delta G_{X/solv}$ and $\Delta G_{Y/solv}$. If mutation of Y allows water to bind to X and vice versa, $\Delta G_{X/solv}$ and $\Delta G_{Y/solv}$ are the energies of the hydrogen bonds with water. Equation A17 then measures the free energy change for the process of $X\cdots H_2O + H_2O\cdots Y \rightleftarrows X\cdots Y + H_2O\cdots H_2O$; that is, the relative energetics of the classical exchange reaction for (intramolecular) hydrogen bonding in water. If there is no access of solvent on mutation of X or Y, then $\Delta G_{X/solv} + \Delta G_{Y/solv}$ in eq A17 is zero and so $\Delta\Delta G_{int} = G_{X/Y}$.

Similar schemes may be applied to measure other interactions.

Measurement of Interaction Energies from Free Energies of Unfolding. $\Delta\Delta G_{int}$ in the above refers to interactions in the folded state. In practice, however, $\Delta\Delta G_{int}$ is measured from changes in unfolding or folding energies $[\Delta\Delta\Delta G_{int(fold)}]$. $\Delta\Delta\Delta G_{int(fold)}$ may be related to $\Delta\Delta G_{int}$ as follows. An identical analysis of eq A1–A17 is applied to the unfolded state, and the free energies of the unfolded state (ΔG_U) are substracted from those in the folded state (ΔG_F). It is then seen that $\Delta\Delta\Delta G_{int(fold)} = \Delta\Delta G_{intF} - \Delta\Delta G_{intU}$. In most cases, the double-mutant interaction energy in the unfolded state, $\Delta\Delta G_{intU}$, is zero since the residues X and Y do not, in general, interact in the random coil. This is true for short-range interactions like hydrogen bonding. Coulombic interactions are of longer range but the interactions between X^+ and Y^- in the unfolded proteins should be small because of large distances between residues that are not contiguous in a fluctuating random coil.

A further factor is that denaturation is often induced by a denaturant, such as urea. Earlier studies on barnase have shown that the energetics of unfolding agree within experimental error for measurements from urea, guanidinium chloride, or temperature-induced denaturation (Kellis et al., 1989). Use of eq 4 to calculate the value of $\Delta\Delta G_{H_2O}$ ($\Delta\Delta G_{H_2O} = \langle m\rangle\Delta[U]_{50\%}$) between wild type and a mutant could lead

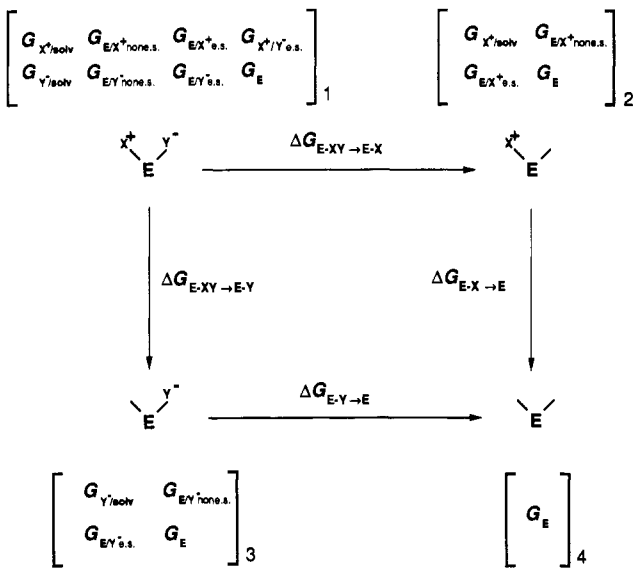

FIGURE 3: Double-mutant cycle for two charged residues, X^+ and Y^-. The free energy terms for each state are given in parentheses, with a numeric subscript referring to each state. $G_{X^+/solv}$ is the interaction energy of X^+ with solvent; G_{E/X^+nones} is the nonelectrostatic interaction energy of X^+ with E (apart from that with Y^-); G_{E/X^+es} is the electrostatic (coulombic) energy between X^+ and E (apart from that with Y^-); G_{X^+/Y^-es} is the electrostatic energy between X^+ and Y^-; G_E is the interaction energy within the protein and solvent shell other than that with X^+ and Y^-. Similar definitions apply to terms involving Y^-.

to errors if the value of m changes on mutation. If m does change, the calculated value of $\Delta\Delta G$ is the one that is correct for the concentration of urea ($\langle[U]\rangle$) that is the arithmetic mean of the values of $[U]_{50\%}$ for the two enzymes studied. This will differ slightly from $\Delta\Delta G_{H_2O}$, the value in the absence of urea. It may be shown from a simple thermodynamic cycle that $\Delta\Delta G_{H_2O} = \Delta\Delta G_{\langle[U]\rangle} + \delta\Delta\Delta G$, where $\delta\Delta\Delta G$ is the difference in free energy of transfer from water to $\langle[U]\rangle$ M urea of the wild-type and mutated side chains, allowing for their degree of exposure to solvent in the folded and unfolded states [cf. Tanford (1969)]. For fully exposed surface residues, $\delta\Delta\Delta G$ is zero because there is no change in exposure of the side chains on denaturation. If the relevant side chains are fully buried in the folded state and fully exposed in the denatured, then this could lead to errors in $\Delta\Delta G_{H_2O}$ for a single mutation in the region of a few tenths of a kilocalorie per mole at $\langle[U]\rangle \sim 4$ M according to the data of Nozaki and Tanford (1963) on the free energies of transfer of groups from water to urea. But these errors cancel out when calculating $\Delta\Delta G_{int}$ from the double-mutant cycles when $\langle[U]\rangle$ is similar for the parallel sides of the cycle (e.g., for $\Delta G_{E\text{-}XY \rightarrow E\text{-}Y}$ and $\Delta G_{E\text{-}X \rightarrow E}$ in Figure 3). The value of $\Delta\Delta G_{int}$ from such double-mutant cycles is that pertaining to $[U] = \langle[U]\rangle$.

Registry No. Barnase, 37300-74-6.

REFERENCES

Aue, W. P., Bartholdi, E., & Ernst, R. R. (1976) *J. Chem. Phys. 64*, 2229–2246.

Bax, A., & Freeman, R. (1981) *J. Magn. Reson. 44*, 542–561.

Bycroft, M., Sheppard, R. N., Lau, F. T.-K., & Fersht, A. R. (1990) *Biochemistry 29*, 7425–7432.

Carter, P. J., Winter, G., Wilkinson, A. J., & Fersht, A. R. (1984) *Cell 38*, 835–840.

Chang, A. C. Y., & Cohen, S. N. (1978) *J. Bacteriol. 134*, 1141–1156.

Cupo, J. E., & Pace, C. N. (1983) *Biochemistry 22*, 2654–2658.

Fersht, A. R. (1987) *Trends Biochem. Sci. 12*, 301–304.

Fersht, A. R. (1988) *Biochemistry 27*, 1577–1580.

Fersht, A. R., & Sternberg, M. J. E. (1989) *Protein Eng. 2*, 527–530.

Grodberg, J., & Dunn, J. J. (1988) *J. Bacteriol. 170*, 1245–1253.

Hartley, R. W. (1975) *Biochemistry 14*, 2367–2370.

Hartley, R. W. (1989) *Trends Biochem. Sci. 14*, 450–454.

Hartmann, H., Jaenicke, R., & Lertes, E. (1967) *Z. Naturforsch. 22A*, 1652–1654.

Hill, C., Dodson, G., Heinemann, U., Saenger, W., Mitsui, Y., Nakamura, K., Borisov, S., Tischenko, G., Polyakov, K., & Pavlovsky, S. (1983) *Trends Biochem. Sci. 8*, 364–369.

Hol, W. G. J. (1985) *Prog. Biophys. Mol. Biol. 45*, 149–195.

Horovitz, A. (1986) *Proc. R. Soc. London, Ser. B 229*, 315–329.

Horovitz, A. (1987) *J. Mol. Biol. 196*, 733–735.

Jeener, J., Meier, B. H., Bachmann, P., & Ernst, R. R. (1979) *J. Chem. Phys. 71*, 4546–4553.

Kauzmann, W. (1959) *Adv. Protein Chem. 14*, 1–63.

Kellis, J. T., Jr., Nyberg, K., Sali, D., & Fersht, A. R. (1988) *Nature 33*, 784–786.

Kellis, J. T., Jr., Nyberg, K., & Fersht, A. R. (1989) *Biochemistry 28*, 4914–4922.

Kumar, A., Ernst, R. R., & Wüthrich, K. (1980) *Biochem. Biophys. Res. Commun. 95*, 1–6.

Lennox, E. (1955) *Virology 1*, 190–206.

Marqusee, S., & Baldwin, R. L. (1987) *Proc. Natl., Acad. Sci. U.S.A. 84*, 8898–8902.

Matouschek, A., Kellis, J. T., Serrano, L., & Fersht, A. R. (1989) *Nature 340*, 122–126.

Mauguen, Y., Hartley, R. W., Dodson, E. J., Dodson, G. G., Bricogne, G., Chothia, C., & Jack, A. (1982) *Nature 297*, 162–164.

Mossakowska, D. N., Nyberg, K., & Fersht, A. R. (1989) *Biochemistry 28*, 3843–3850.

Nicholson, H., Becktel, W. J., & Matthews, B. W. (1988) *Nature 336*, 651–656.

Nozaki, Y., & Tanford, C. (1963) *J. Biol. Chem. 238*, 4074–4081.

Pace, C. N. (1986) *Methods Enzymol. 131*, 266–279.

Paddon, C. J., & Hartley, R. W. (1987) *Gene 53*, 11–19.

Pavlovsky, A. G., Vagin, A. A., Vainstein, B. K., Chepurnova, N. K., & Karpeisky, M. Ya. (1983) *FEBS Lett. 162*, 167–170.

Pavlovsky, A. G., Sanishvili, R. G., Borisova, S. N., Strokopytov, B. V., Vagin, A. A., Chepurnova, N. K., & Vainstein, B. K. (1989) *Krystallografiya (USSR) 34*, 137–142.

Perutz, M. F. (1978) *Science 201*, 1187–1191.

Russell, A. J., & Fersht, A. R. (1987) *Nature 328*, 496–500.

Russell, A. J., Thomas, P. G., & Fersht, A. R. (1987) *J. Mol. Biol. 193*, 803–813.

Sali, D., Bycroft, M., & Fersht, A. R. (1988) *Nature 335*, 741–743.

Sanishvili, R. G. (1989) Ph.D. Thesis, Moscow University, Moscow.

Sayers, J. R., & Eckstein, F. (1988) in *Genetic Engineering: Principles and Methods* (Setlow, J. K., Ed.) Vol. 10, p 109, Plenum Press, New York and London.

Serpersu, E. H., Shortle, D., & Mildvan, A. S. (1986) *Biochemistry 25*, 68–87.

Serrano, L., & Fersht, A. R. (1989) *Nature 342*, 296-299.
Shoemaker, K., Kim, P. S., York, E. J., Stewart, J. M., & Baldwin, R. L. (1987) *Nature 326*, 563-567.
Smeaton, J. R., & Elliott, W. H. (1967) *Biochim. Biophys. Acta 145*, 547-560.
Studier, F. W., & Moffatt, B. A. (1986) *J. Mol. Biol. 189*, 113-130.
Tanford, C. (1969) *Adv. Protein Chem. 24*, 1-95.
Thomas, D. G., Russell, A. J., & Fersht, A. R. (1985) *Nature 318*, 375-376.
Warshel, A., & Russel, S. T. (1984) *Q. Rev. Biophys. 17*, 283-422.

Purification of Recombinant Ribulose-1,5-bisphosphate Carboxylase/Oxygenase Large Subunits Suitable for Reconstitution and Assembly of Active L_8S_8 Enzyme†

Bonggeun Lee and F. Robert Tabita*
Department of Microbiology and The Biotechnology Center, The Ohio State University, 484 West 12th Avenue, Columbus, Ohio 43210
Received April 18, 1990; Revised Manuscript Received July 9, 1990

ABSTRACT: Ribulose-1,5-bisphosphate carboxylase/oxygenase (RubisCO) from *Anacystis nidulans* was reconstituted in vitro from extracts of *Escherichia coli* strains that separately express large and small subunits. This reconstitution system was shown to be useful for monitoring the appearance of dissociated or fractionated subunit preparations. Recombinant large subunits were purified to a state of homogeneity and retained reconstitution capacity in the presence of added small subunits. The purified large subunits appeared to be in the form of an octamer, probably an L_8 structure, and showed 0.15% of the carboxylase activity of the purified L_8S_8 enzyme. Purified large subunit octamers are disrupted by nondenaturing PAGE; however, the octamer is stable to electrophoresis in the presence of exogenous protein.

Ribulose-1,5-bisphosphate (RuBP) carboxylase/oxygenase (RubisCO)[1] is an important enzyme which catalyzes the initial reaction of the two competing metabolic pathways of photosynthetic CO_2 fixation and photorespiratory carbon oxidation (Tabita, 1988). This bifunctional enzyme catalyzes both the carboxylation and the oxygenation of RuBP. Considerable research on this enzyme has given productive information about its catalysis and structure (Andrews & Lorimer, 1987). In plants, algae, and most bacteria, RubisCO is a hexadecameric protein (L_8S_8) which is composed of eight large subunits of about 55 kDa and eight small subunits of about 13 kDa. While the large subunit bears the sites for activation and catalysis, the role of the small subunit is not fully understood despite its requirement for full enzyme activity (Andrews & Ballment, 1983). In the case of the L_8S_8 enzyme, the small subunits are attached to the top and the bottom of the large subunit octamer (Andersson et al., 1989; Chapman et al., 1988). In plants and green algae, the large and small subunits are encoded by the chloroplast and nuclear genomes, respectively. Unlike the situation in most eucaryotic organisms, the large and small subunit genes of RubisCO from the cyanobacterium *Anacystis nidulans*, which performs an oxygenic photosynthesis, are linked together and cotranscribed (Shinozaki & Sugiura, 1985). Because of the procaryotic nature of the *Anacystis* RubisCO genes, active and correctly assembled recombinant hexadecameric enzyme may be synthesized in *Escherichia coli* (Christeller et al., 1985; Gatenby et al., 1985; Tabita & Small, 1985). When the large subunit gene was separately expressed in *E. coli*, large subunits were synthesized, presumably in the form of L_8 octamers (Andrews, 1988). This crude L_8 RubisCO showed weak but measurable RubisCO activity; however, the protein was labile and resisted further attempts at purification.

In this investigation, we have shown that recombinant large and small subunits from separately expressed *rbcL* and *rbcS* genes of *A. nidulans* were active in reconstitution of RubisCO activity in vitro. Furthermore, the large subunits were purified to homogeneity in a stable L_8 form.[2]

Experimental Procedures

Bacterial Strains and Plasmids. *E. coli* strain MV1190 [Δ(*lac-pro* AB), *thi*, *sup* E, Δ(*srl-recA*)306::Tn10(tet^r)[F′*tra* D36, *pro* AB, *lac*I^{q}ZΔM15])] was used as the host strain for plasmids employed in this study. Plasmids constructed for this study were derived from plasmid pCS75 (Tabita & Small, 1985). *E. coli* MV1190 was purchased from Bio-Rad, Richmond, CA. Plasmids pTZ18R (Mead et al., 1986), pUC9 (Vieira & Messing, 1982), and pUC18 (Yanisch-Perron et al., 1985) were used as vectors for cloning.

Cell Culture and Preparation of Crude Extracts. *E. coli* plasmid-containing strains were grown for 8-9 h in Luria-Bertani medium (Maniatis et al., 1982) containing 100 μg/mL ampicillin; 5 mL of this culture was used to inoculate 1 L of Luria-Bertani medium containing 100 μg/mL ampicillin. This

† This work was supported by a grant from the National Institutes of Health (GM-24497).
* Correspondence should be addressed to this author at the Department of Microbiology, The Ohio State University.

[1] Abbreviations: RubisCO, ribulose-1,5-bisphosphate carboxylase/oxygenase; IPTG, isopropyl β-D-thiogalactopyranoside; TEM, 25 mM Tris-HCl, pH 8.0, 1 mM EDTA, and 5 mM β-mercaptoethanol; TEMMB, 25 mM Tris-HCl, pH 8.0, 1 mM EDTA, 5 mM β-mercaptoethanol, 10 mM $MgCl_2$, and 50 mM $NaHCO_3$; SDS-PAGE, sodium dodecyl sulfate-polyacrylamide gel electrophoresis; DPM, disintegrations per minute; L, large subunit(s); S, small subunit(s).

[2] A preliminary report of this work has appeared (Tabita, 1989).

0006-2960/90/0429-9352$02.50/0